Mechanism for enhanced oxygen reduction kinetics at the $(La,Sr)CoO_{3-\delta}/(La,Sr)_2CoO_{4+\delta}$ hetero-interface

Jeong Woo Han and Bilge Yildiz*

Laboratory for Electrochemical Interfaces, Department of Nuclear Science and Engineering, Massachusetts Institute of Technology,
77 Massachusetts Avenue, Cambridge, Massachusetts 02139, USA

Supplementary Information

I) Supplementary discussion on the effects of surface coverage and Sr-content:

Surface coverage effect: Calculations for adsorbed O_2 molecule were performed for a coverage corresponding to one molecule per surface unit cell. Since there are four equivalent sites of O_2 adsorption in our surface unit cell, this corresponds to the O_2 surface coverage of 25%. Using the calculations with smaller surface coverage of 12.5%, we tested if there is an artificial coverage effect due to the supercell size on the adsorption energy. But we found that there is no dramatic difference in coverage effect with 0 and 50% Sr-doping .

Possible reason for the large adsorption energy on undoped LSC_{214}(100) compared to 50% Sr-doped one: Section 3.1.2, we explained that more significant surface relaxation on undoped LSC_{214}(100) is a main reason of the larger adsorption energy compared to 50% Sr-doped one. To quantify role of surface relaxation in adsorption strength, we computed the energy required for surface deformation/relaxation upon O2 adsorption. This can be defined as the difference between the total energy of the optimized structure of the bare surface and the surface in the same geometry as the adsorbed structure but with no O_2 present. The surface relaxation energy of 2.43 eV is required upon the O_2 adsorption on undoped LSC_{214}(100), while that of 0.87 eV on 50% Sr-doped LSC_{214}(100). This confirms that to strongly accommodate the adsorbing O_2, the undoped surface does significantly relax and deform, but due to the large Sr atoms 50% Sr-doped LSC_{214}(100) does not, resulting in a much lower O_2 adsorption energy.

* Corresponding author. Email: byildiz@mit.edu

II) Oxygen diffusion on LSC_{214}(100) surface:

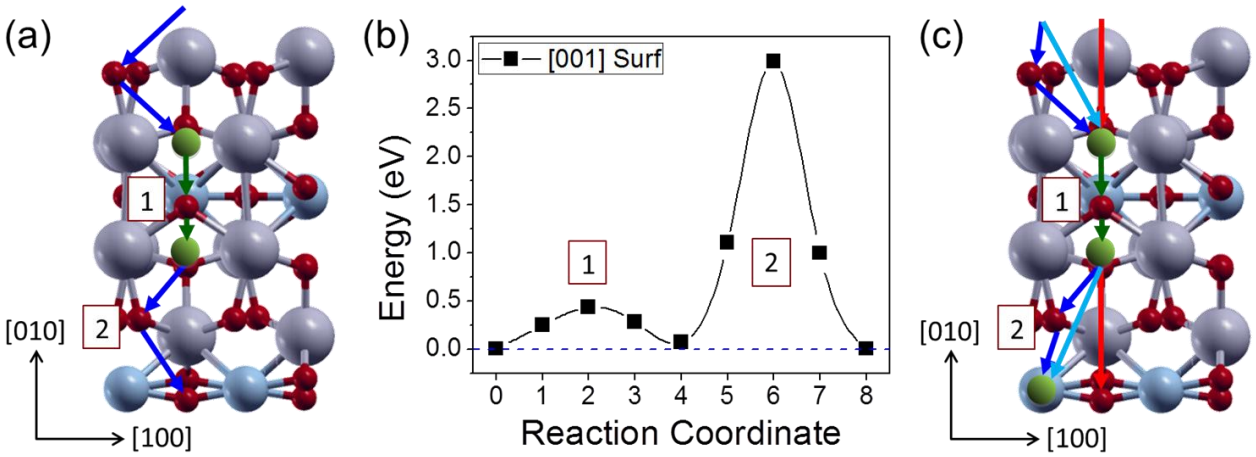

Figure S1: (a) The minimum energy path found for the oxygen migration on LSC_{214}(100) surface, (b) the energy surface of the oxygen migration path shown in (a), and (c) three other paths of oxygen migration that were considered, but with higher effective barrier than in (a).

Unlike the migration of oxygen in the bulk LSC_{214}, the migration on the LSC_{214}(100) surface occurs via two steps (marked as 1 and 2 in Fig. S1). Similarly to the migration in the bulk, in part 1, the oxygen replaces the lattice oxygen of the surface by kicking it off into the neighboring oxygen adsorption site (as shown with green arrows in Fig. S1(a)). For the part 2, the oxygen migrates via the three steps of exchange mechanisms. The migrating oxygen consecutively replaces its nearest lattice oxygen by kicking it off into the nearest lattice oxygen position. For part 2, we also considered three other possible paths as shown in Fig. S1(c), but they all showed higher energy barriers than the path shown in Fig. S1(a)).

III) Sr distribution in LSC_{214}

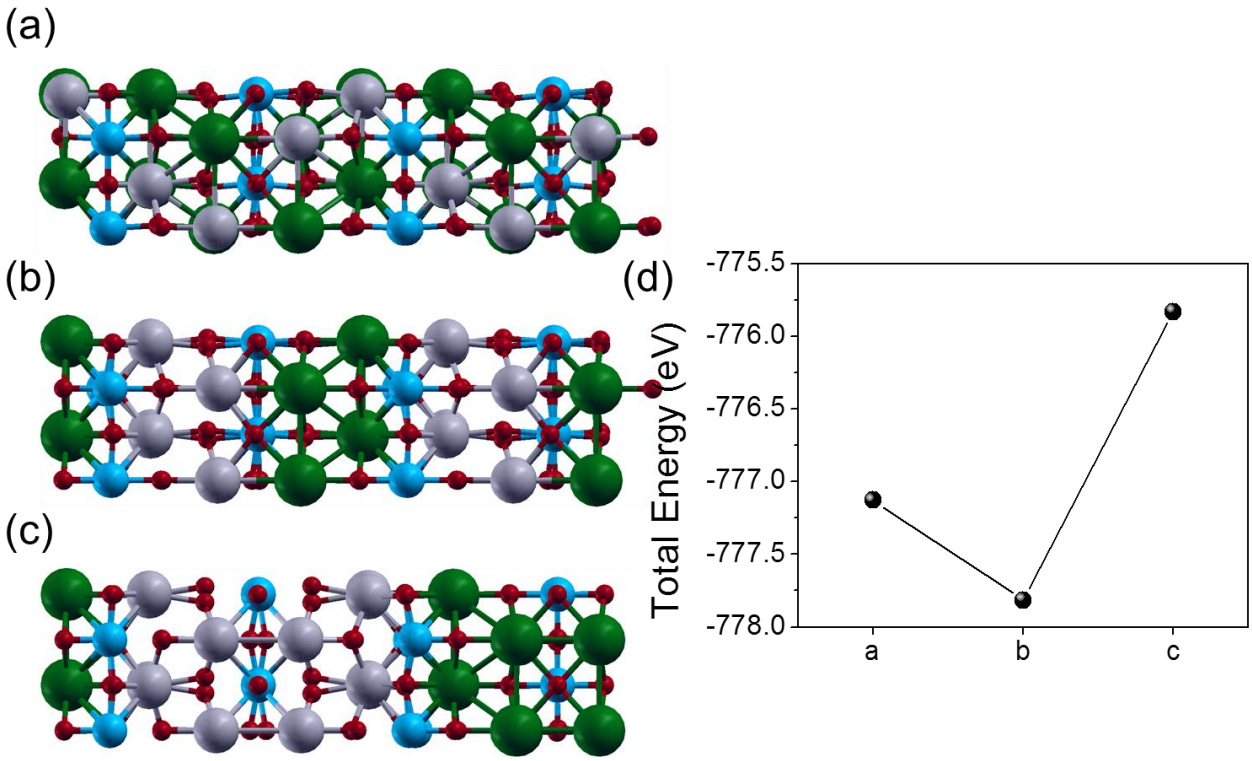

Figure S2: (2×1) 50% Sr-doped LSC_{214} models with (a) a uniform distribution of Sr, (b) cation ordered double layers of SrO and LaO, 2:2 ordered perpendicular to the *c* axis, (c) cation ordered double layers of SrO and LaO 4:4 ordered perpendicular to the *c* axis, and (d) their corresponding total energies. The configuration (b) is more stable than (a) by 0.04 eV/formula unit (f.u.) and (c) by 0.12 eV/formula unit (f.u.), respectively.

IV) Oxygen vacancy and interstitial formation in the bulk and on the surface of LSC_{214}:

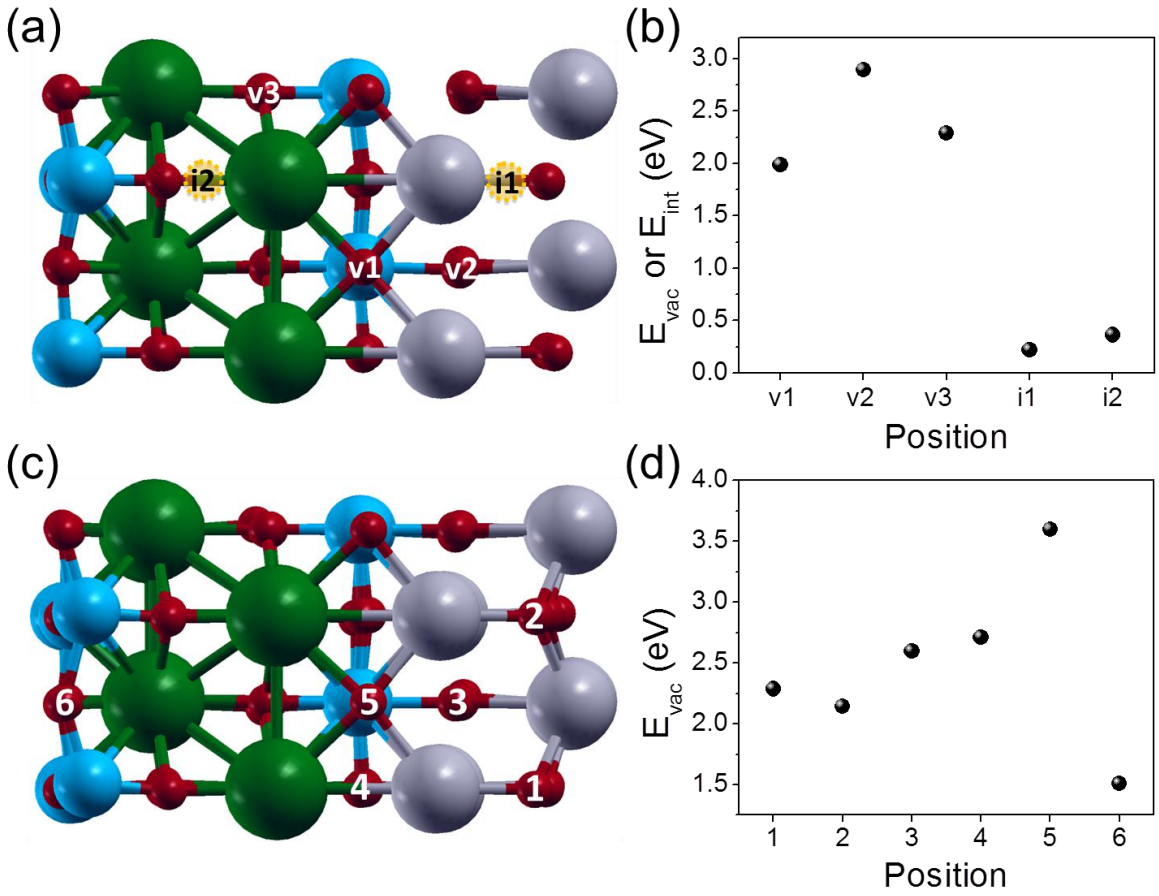

Figure S3: (a) The positions of oxygen vacancies (v) and interstitials (i), and (b) their formation energies in the bulk 50% Sr-doped LSC_{214}. (c) The positions of oxygen vacancies, and (d) their formation energies on the 50% Sr-doped LSC_{214}(100) surface.

The vacancy and interstitial formation energies at various positions were explored for the surface and bulk of 50% Sr-doped LSC_{214}. In bulk LSC_{214}, the oxygen interstitial formation energy (E_{int} = 0.22 eV) is much lower than the oxygen vacancy formation energy (E_{vac} = 2 eV). For the LSC_{214} (100) surface, while the position 6 has the lowest vacancy formation energy (1.51 eV), this is not the favorable oxygen adsorption and incorporation site because atomic oxygen diffusion (with energy barrier of 2.06 eV) toward the incorporation channel near the LaO-LaO rock-salt plane is required as shown in Fig. S4(e). The favorable site of oxygen adsorption and direct incorporation on the LSC_{214} surface is the position 2, whose vacancy formation energy is 2.15 eV.

V) Oxygen incorporation pathways on 50% Sr-doped LSC_{214}(100)

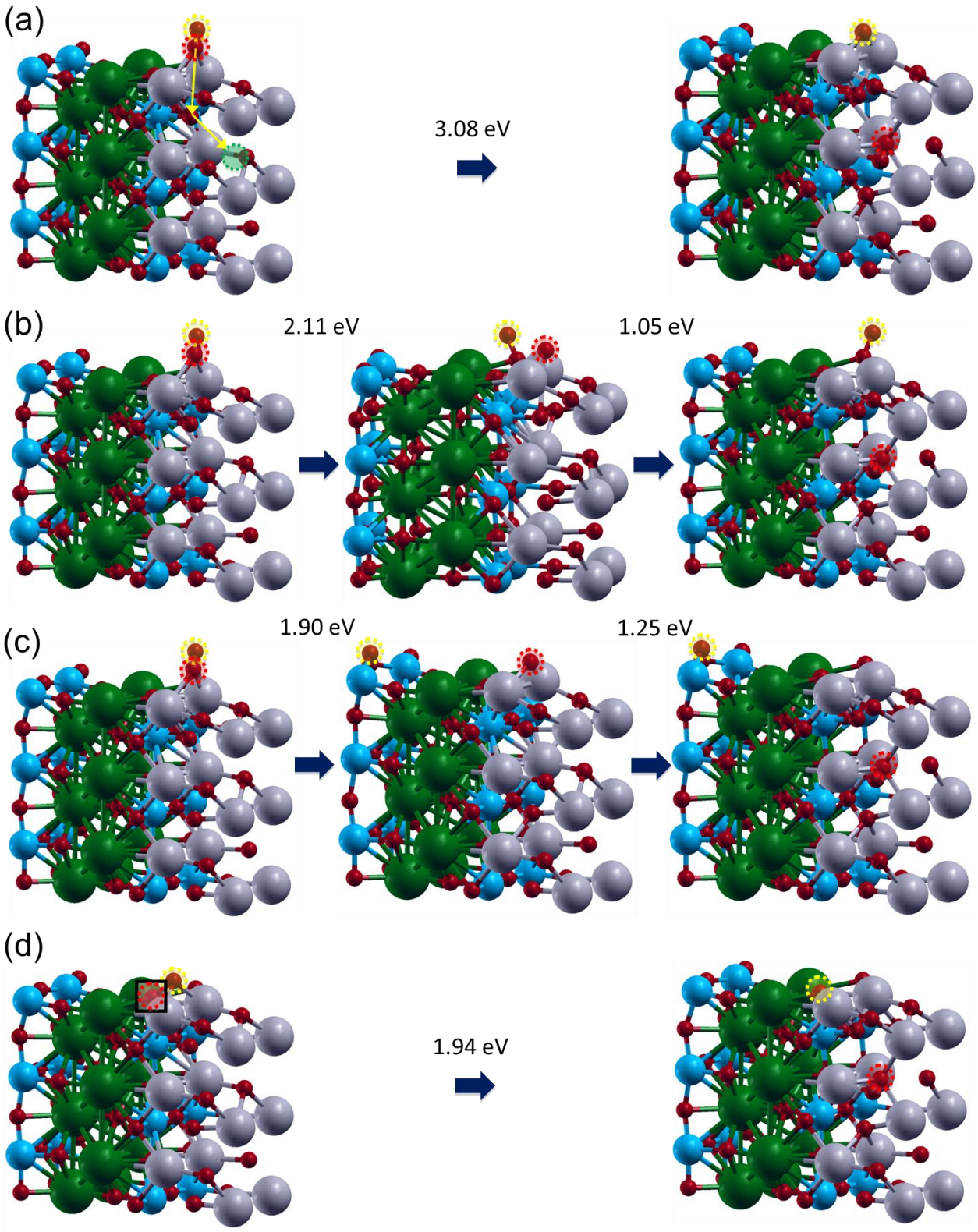

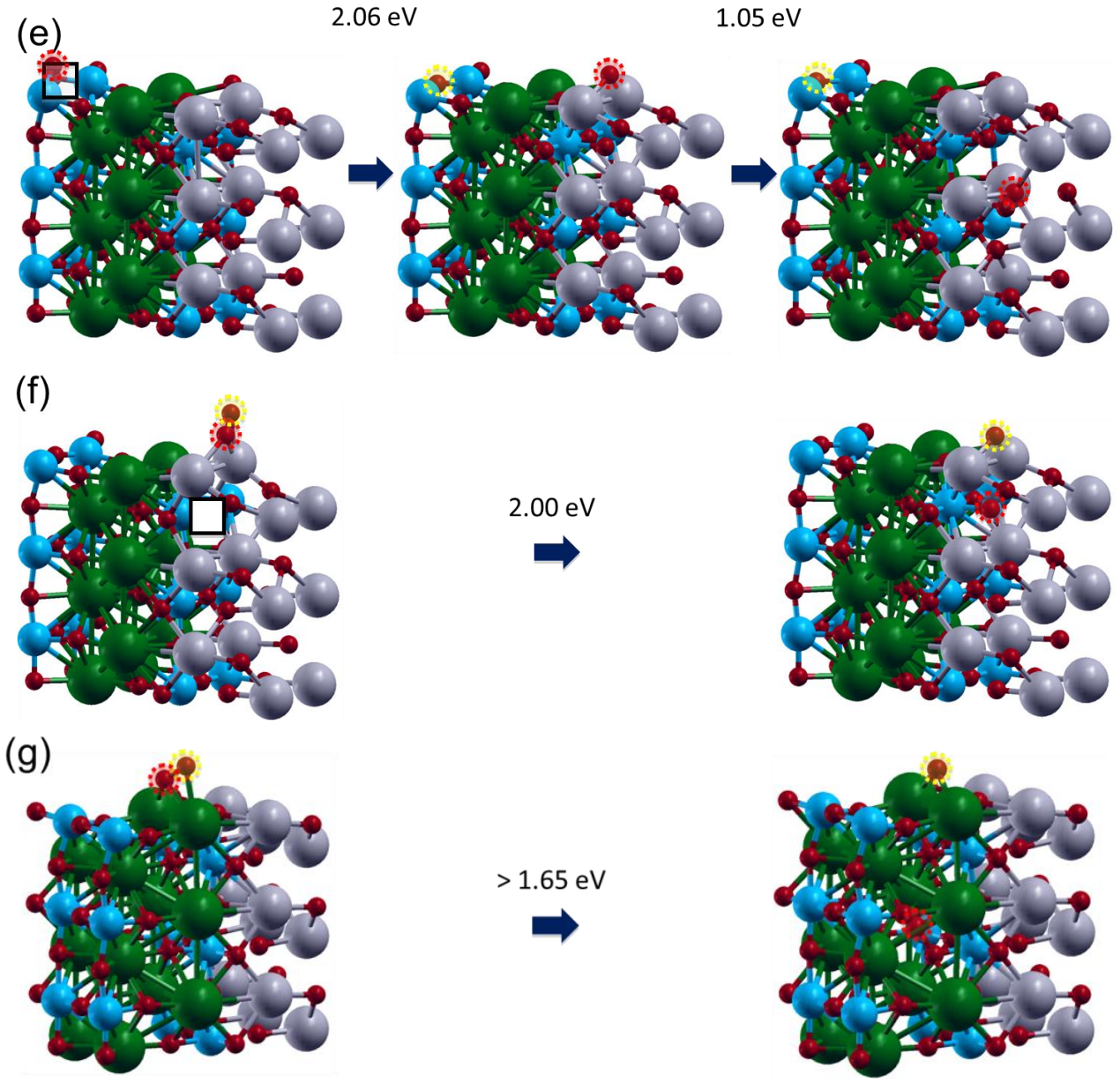

Figure S4: Eight possible oxygen incorporation pathways were investigated on 50% Sr-doped LSC_{214}(100) (including the energetically most favorable one shown in Fig. 4(c) and the insets of Fig. 4(d) in the paper). The site at which an oxygen vacancy was created is shown with a square. The adsorption and dissociation of the oxygen are shown with yellow and red dashed circles.

(a) An O_2 molecule adsorbs onto the bridge site between La atoms in the vicinity of the interstitial path between the LaO planes as shown in Fig. 4(a). Similarly to the incorporation pathway on the undoped LSC_{214}(100) (Fig. 3(c) and the insets of Fig. 3(d)), the O_2 adsorption on

the surface is followed by rotation and dissociation of O_2 that directly leads to O incorporation as an interstitial into the rock-salt layer by interstitialcy mechanism. The surface vacancy is not involved, and the dissociation/incorporation with a barrier of 3.08 eV is the limiting step in this process.

(b)-(c) O_2 dissociates from its adsorption site near the rock-salt layer (no vacancies are involved) . The dissociated atomic O then diffuses onto the bridge site between La atoms in the vicinity of the interstitial path between the LaO planes. After this, the atomic O incorporates into the LaO-LaO rock-salt layers. The difference between (b) and (c) is the position of an atomic O after the dissociation reaction. For (b), the dissociated atomic O diffuses out towards the nearest bridge site between Sr atom and La atom, while for (c) it moves towards the bridge site between Co atom and O atom on the CoO_2 layer. In addition, this atomic O that diffused away should migrate again to a bridge site near the LaO rock-salt layer for the incorporation, and overcome the diffusion barrier of 1.08 eV for (b) and 2.06 eV for (c), respectively. The limiting high-barrier step for (b) is the O_2 dissociation reaction step on the surface (2.11 eV), but the one for (c) is the O diffusion (2.06 eV).

(d) The O_2 molecule adsorbs into the surface vacancy 5 in Fig. S3(c), and then dissociates and incorporates into the interstitial site between the LaO planes. Before this process, the surface oxygen vacancy should be created at the position 5 in Fig. S3(c), but the formation energy is very high (3.60 eV in Fig. S3(d)), which is the limiting step for this pathway.

(e) This pathway involves a surface vacancy near the CoO layer, which has the lowest formation energy (position 6 in Fig. S3(c)), but this requires an additional (and limiting step) of atomic O diffusion (with the barrier of 2.06 eV) toward the incorporation channel near the LaO-LaO rock-salt plane.

(f) The oxygen vacancy is at the lattice oxygen just below the LaO-LaO bridge site. Although this vacancy reduces the dissociation/incorporation barrier to 2.00 eV from the one (3.08 eV) in (a) for the same process, it requires a vacancy formation energy of 2.60 eV, which is the limiting step for this pathway.

(g) This pathway is similar to the one in (a), but the oxygen adsorption and dissociation / incorporation processes occur near the SrO-SrO rock-salt layers. The final state in which oxygen dissociates and incorporates into the interstitial site between the SrO planes is less stable than the

initial state in which O_2 is adsorbed by 1.65 eV. So we did not further calculate the barrier for the dissociation/incorporation because it is expected to be far more than 1.65 eV.

Among the eight pathways explored, the one shown in Fig. 4(c) and the insets of Fig. 4(d) of the paper is energetically the most favorable. An O_2 first adsorbs into a surface vacancy on the rock-salt layer at the position 2 in Fig. S3(c), followed by oxygen dissociation and incorporation into an interstitial site in the rock-salt layer. The creation of surface oxygen vacancy requires 2.15 eV and the oxygen dissociation and incorporation barrier is 0.83 eV. The limiting step for this pathway is the surface vacancy formation.

(eV)	$E_{adsorption}$	$E_{dissociation}$	$E_{incorporation}$	$E_{diffusion}$	E_{tot}
(a)	-0.81	-	3.08	-	2.27
(b)	-0.81	2.11	1.05	1.08	3.43
(c)	-0.81	1.90	1.25	2.06	4.40
(d)	-3.99	3.60	1.94	-	1.55
(e)	-1.60	1.51	1.05	2.06	3.02
(f)	-0.81	2.60	2.00	-	3.79
(g)	-0.40	-	> 1.65	-	> 1.25
Most favorable	-2.02	2.15	0.87	-	0.99

Table S1. The energetics for each unit process and the corresponding E_{tot} for each pathway are summarized. E_{tot} denotes the sum of the energetics required for the oxygen adsorption and incorporation.

VI) Strain dependence of LaO-LaO channel opening

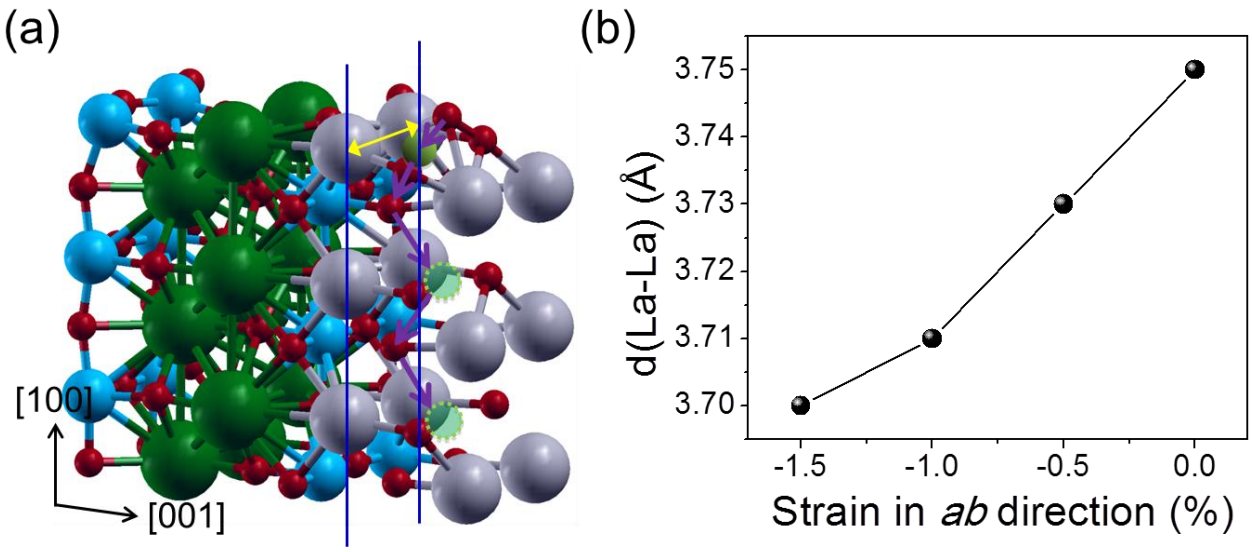

Figure S5: (a) La-La distance, *d*(La-La) (yellow arrow), is quantified to represent the space available to incorporate oxygen interstitials into LSC_{214}(100) surface. (b) Strain dependence of the *d*(La-La) on LSC_{214}(100).

VII) Potential energy diagram of the surface reaction steps on $LSC_{214}(100)$:

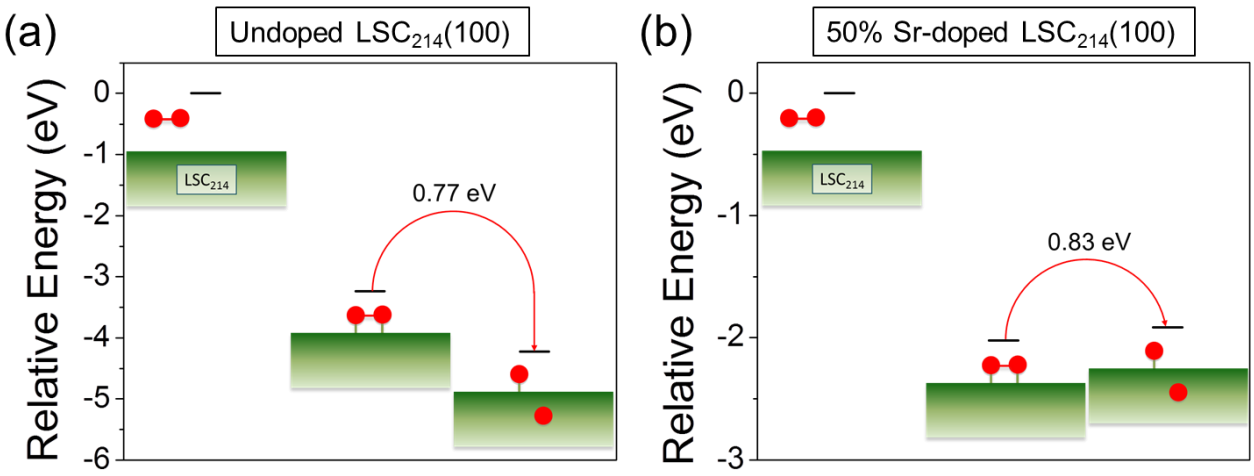

Figure S6: Potential energy diagram of the reaction steps from the gaseous O_2 to the O incorporation into the LSC_{214}: (a) undoped $LSC_{214}(100)$ and (b) 50% Sr-doped $LSC_{214}(100)$, with respect to the same reference state (O_2 in gas phase).

VIII) Bond length and charge analysis:

	Undoped $LSC_{214}(100)$	**50% Sr-doped $LSC_{214}(100)$**
Bond Length (Å)	2.33, 2.38, 2.40, 2.41	2.35, 2.39, 2.50, 2.54
O_2 effective charges (e)	-1.69	-1.41

Table S2. Bond length and effective charge (by Bader charge analysis) of the adsorbed O_2 on the undoped and 50% Sr-doped $LSC_{214}(100)$. As shown in Fig. 3(a) and 4(a) in the paper, the O_2 molecule adsorbs on the surface through four bonds with the nearest La atoms.

The O_2 bond length and effective charges can serve as a measure of the adsorption strength. We showed in the manuscript that the O_2 adsorption energy on undoped $LSC_{214}(100)$ is greater than the one on 50% Sr-doped one. Consistent with this finding, the bond length on undoped $LSC_{214}(100)$ is shorter than the one on 50% Sr-doped one, and the O_2 effective charges on undoped $LSC_{214}(100)$ is larger than the one on 50% Sr-doped one as shown in Table S2.